Magnetization and ^{63}Cu NMR studies on granular FeCu alloys

B. Bandyopadhyay, B. Pahari, and K. Ghoshray
Saha Institute of Nuclear Physics, 1/AF Bidhannagar, Kolkata 700 064, India
(Received 29 March 2007; revised manuscript received 26 July 2007; published 26 December 2007)

Nanostructured FeCu granular alloys (Fe ~1%–20%) have been prepared by borohydride reduction and characterized by energy dispersive spectroscopy, x-ray, and transmission electron microscopy studies. Study of zero-field-cooling–field-cooling magnetization yields blocking temperature distribution of magnetic fine particles system in all samples. At low Fe concentration, the magnetizations of the samples combine superparamagnetism and paramagnetism near room temperature and small hystereses at 5 K. High Fe content alloys are almost entirely ferromagnetic even at 300 K. However, in all these samples, the observation of the ^{63}Cu nuclear magnetic resonance signal at all temperatures 4–300 K confirms the existence of a paramagnetic component having ~0.02–0.04 at. % Fe in Cu. The temperature dependence behavior of Fe contribution to ^{63}Cu NMR linewidth and the Knight shift indicate that the paramagnetic component might exhibit a Kondo temperature of ~24 K that is significantly higher than that obtained in bulk dilute FeCu alloys.

DOI: 10.1103/PhysRevB.76.214424 PACS number(s): 75.75.+a, 76.60.−k

I. INTRODUCTION

The observation of giant magnetoresistance in granular CoCu system[1,2] initiated extensive studies on the production and characterization of binary alloys combining a ferromagnetic transition metal with Cu or Mn, or with noble metals. Such combinations are often characterized by high enthalpies of mixing, but metastable alloys at any ratio between the two metals can be produced by various procedures, e.g., vapor quenching,[3–8] ball milling,[9,10] electrodeposition,[11] and chemical reduction.[12–14] The last method, that is, how the samples were prepared in this study, may ensure a good chemical homogeneity of the alloy as nanometer size alloy particles are produced by simultaneous reduction of ions of the constituent metals from a mixture of solutions of their salts.

In magnetic nanoparticles, the correlation lengths of both the anisotropy and the exchange interaction typically coincide with the grain size. These factors together with the long range magnetic dipolar and Ruderman-Kittel-Kasuya-Yosida (RKKY) interactions determine the ground state magnetic properties of such systems which are often described as spin-glass or disordered materials. However, the exchange interaction, which is of a local character, can also propagate through the atoms at the boundaries of the particles leading to a long range magnetic order. The bulk magnetic properties such as susceptibility and coercivity are determined by local parameters, e.g., size and composition of particles and clusters. Both macroscopic and microscopic characterizations are therefore necessary to understand the magnetic properties of nanoparticles.

We have prepared FeCu granular alloys (Fe ~1%–20%) by chemical reduction and characterized the samples by x-ray diffraction, energy dispersive spectroscopy (EDS), and transmission electron microscopy (TEM). Magnetic properties have been studied macroscopically and also using ^{63}Cu nuclear magnetic resonance (NMR) as a local probe.

II. SAMPLE PREPARATION AND CHARACTERIZATION

Oxygen was removed from double distilled water by bubbling argon and stirring for over 12 h. Mixtures of aqueous $FeCl_2$ (Alfa Aesar) and $CuCl_2$ (Merck) solutions of equal volumes (30 ml) and different molar concentrations in the desired ratio were made so that the total metal ion concentration in the mixture remained at 1*M*. A volume of 15 ml of 2.5*M* aqueous $NaBH_4$ (Lancaster) solution was added dropwise from a burette to the mixture which was kept at room temperature on a magnetic stirrer. At the end of reaction, the temperature of the solution rose by 30 °C and *p*H dropped from a value of ~1.5 to ~0.3, slightly varying upon the initial mixture. The black solid precipitates were thoroughly washed with water, rinsed with acetone, and dried in vacuum at room temperature. In order to prevent oxidation, the dry powders were mixed with epoxy for x-ray and NMR studies. Small (~5 mm^2) pellets were used for EDS and magnetic measurements. TEM studies were performed on sonicated samples.

EDS studies performed with energy dispersive x-ray analysis detector on as-prepared samples show peaks from Cu and Fe, and nothing definitely from Cl or B. A negligibly small peak from oxygen was obtained indicating surface oxidation of pellets. The compositions of the samples are (1) Fe 1.1 at. %, Cu 98.9 at. % (S1); (2) Fe 2.9 at. %, Cu 97.1 at. % (S2); (3) Fe 11.6 at. %, Cu 88.4 at. % (S3); and (4) Fe 20.3 at. %, Cu 79.7 at. % (S4).

Mechanism of borohydride reduction of dissolved metal salts is a combination of several reactions, which, apart from reducing the metal ions, may also yield metal borides and borates.[15–17] The rates of the reactions are determined by various parameters, notably concentrations, BH^{4-}-to-metal ion ratio, *p*H, and the method of mixing. EDS studies found no trace of boron, which is the lightest element detectable by our instrument. Boron gives a strong NMR signal, but no signal could be traced in our samples indicating the absence of borates, paramagnetic metal borides, and elemental boron. However, boron dissolved in the ferromagnetic phase of the intended alloys would not be easily detected due to excessive broadening of NMR signal, and therefore the possibility of such an occurrence of boron is not eliminated.

X-ray studies on all four samples show (Fig. 1) reflections from fcc Cu and none from bcc Fe, suggesting that Fe has

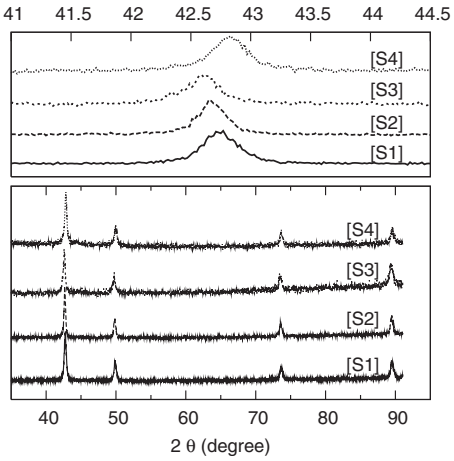

FIG. 1. Room temperature x-ray powder diffraction of S1, S2, S3, and S4. The top panel shows the change in the position of the (111) peak with the Fe content of the samples.

been alloyed in the fcc phase of Cu. It may be noted that the samples are practically free from oxides. The top panel of Fig. 1 shows in an expanded scale the change in position of (111) peak with increasing Fe content. There is a lattice expansion from S1 to S3, and then as Fe concentration is increased further in S4, the lattice parameter is decreased.

Transmission electron micrographs of all the samples were obtained with a Hitachi H600 instrument. The micrographs show spherical particles and hexagonal crystallites as well. Figure 2 shows part of a typical micrograph and the size distribution of the particles as obtained in S2. More than 75% of the particles belong to 5–15 nm diameter. For the same sample, an average particle size of 17 nm were calculated from x-ray data using the Scherrer equation, in which the width B (in radians) of a diffraction peak located at 2θ is related to particle size s as $s=0.9\lambda/B\cos\theta$, and λ is the wavelength of the x-ray. The results are similar for other samples too.

III. RESULTS AND DISCUSSION

A. Magnetic measurements

Magnetic measurements were performed with a Quantum Design superconducting quantum interference device magnetometer. Magnetic susceptibilities, as shown in Fig. 3, were measured under conditions of zero-field cooling (ZFC) and field cooling (FC) with a probing field of 4 mT at tempera-

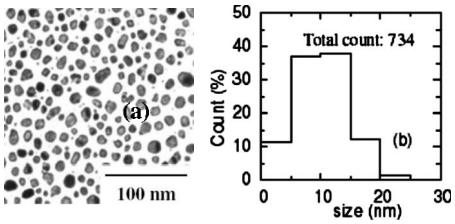

FIG. 2. (a) Transmission electron micrograph and (b) particle size distribution of S2 sample.

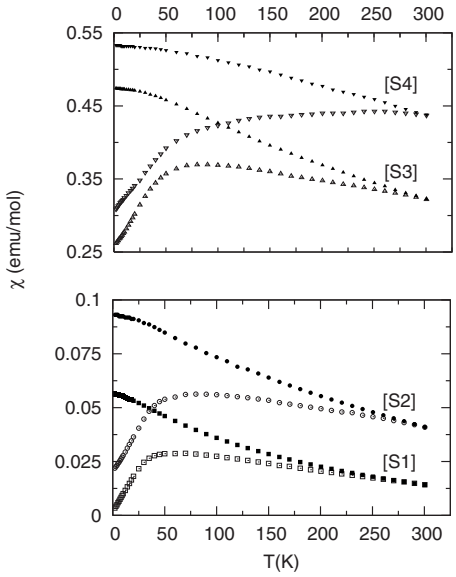

FIG. 3. Zero-field cooled (ZFC, open symbols) and field-cooled (FC, solid symbols) magnetic susceptibilities of S1, S2, S3, and S4, measured with 4 mT probing field.

tures of 2–300 K. The susceptibilities of S1 and S2 are about an order of magnitude less than those of S3 and S4. In ZFC studies, broad maxima centered at 70, 80, and 90 K are achieved for S1, S2, and S3, respectively. In the case of S4, the ZFC magnetization is still increasing at 300 K with no indication of saturation. All samples are thus characterized by some blocking temperature distributions which may reflect variations in particle size and/or chemical inhomogeneities of their compositions. A closer inspection shows that for S1 and S2, the branching in ZFC-FC behavior occur at 260 and 290 K, respectively, indicating that these samples with smaller Fe content are superparamagnetic (SPM) above those temperatures. For S3 and S4, the branching might not have actually taken place below 300 K, and these samples could be ferromagnetic (FM) over the entire range of temperature. The derivative of the difference between ZFC and FC magnetizations (M_{ZFC} and M_{FC}, respectively), or more appropriately, $d[(M_{ZFC}-M_{FC})/M_S]/dT$, where M_S is the saturation magnetization in FC condition, represents the number of particles whose blocking temperature falls into the range of the given temperature.[18,19] The temperature dependences of the normalized derivative for all four samples, i.e., their blocking temperature distribution, are shown in Fig. 4. With an increase in Fe concentration, we observe peak distribution to shift toward higher temperatures. Broad distributions are indicative of particles in a cluster.[24] Magnetization reversal of such clusters usually exhibits substantial coercivity and remanence.

The hysteresis loops were obtained at 300 K and, in ZFC condition, at 5 K in magnetic fields of 0–7 T and were analyzed.[6] S1 and S2 appeared to be SPM as said earlier. However, in addition to SPM contributions, the fittings of their magnetization required addition of small FM contributions also. Moreover, in these two samples, the increase of magnetization at high magnetic fields could be simulated

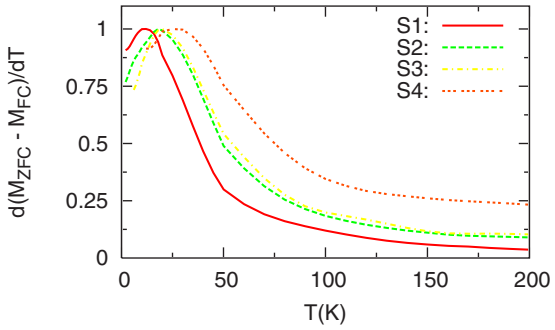

FIG. 4. (Color online) The blocking temperature distributions of samples S1, S2, S3, and S4.

only after incorporating a paramagnetic (PM) component in the fitting equation, as described in the following:

$$M(H) = \frac{2M_S^{FM}}{\pi}\left[\frac{H \pm H_C}{H_C}\tan\left(\frac{\pi M_R^{FM}}{2M_S^{FM}}\right)\right] + M_S^{SPM}\left[\coth\left(\frac{\mu H}{kT}\right) - \left(\frac{\mu H}{kT}\right)^{-1}\right] + C^{PM}H. \quad (1)$$

The first, second, and third terms on the right hand side of the equation represent the FM, SPM, and PM contributions, respectively. M_S^{FM} and M_S^{SPM} are the saturation magnetizations for FM and SPM parts, in terms of magnetic moment per Fe atom. M_R^{FM} is the remanence, H_C the coercivity, and μ the average magnetic moment of SPM particles or clusters. C^{PM} is the susceptibility of the paramagnetic contribution that is linear with the magnetic field H. Experimental data along with fitted curves to Eq. (1) are shown in Fig. 5. The values of H_C and M_R^{FM} were obtained from experiment and required only a little adjustment during fitting. Table I lists various parameters obtained from the fitting of magnetization data for all four samples.

In bulk fcc FeCu alloys with 1.2 at. % Fe, an iron atom carries the full magnetic moment of about 3 μ_B as the first neighbor Fe pairs couple ferromagnetically.[20] For fcc phase of sputtered Fe_xCu_{1-x} alloys of grain size of some tens of nanometers, a negligible moment of Fe atoms was obtained[21] in alloys with $x<10$ at. %. The moment increased monotonically as x increased from about 10 to 40 at. %, with the value of ~ 1 μ_B for $x=21$ at. % that may be compared with our results. It must be mentioned that in S1 and S2, Fe concentrations lie much below the critical concentration obtained from percolation theory for ferromagnetism in a fcc lattice.[22] In ball-milled Fe_xCu_{1-x} alloys, ^{57}Fe Mossbauer studies[23] showed nonmagnetic alloy phases with clustering effects for $x<20$ at. %. The negligible remanences and small values of coercivities in S1 and S2 might also arise due to the formation of clusters where magnetic dipolar and/or RKKY interactions hinder the response of the system of moments to isothermal changes of the applied field.[24]

The magnetization data for S3 and S4, at both 300 and 5 K, could be simulated quite satisfactorily only with the FM component. In vapor deposited 30 nm granular Fe_xCu_{1-x} alloy with $x=20$ at. %, Mossbauer and magnetic measurements yielded[4] a magnetic ordering temperature lower than

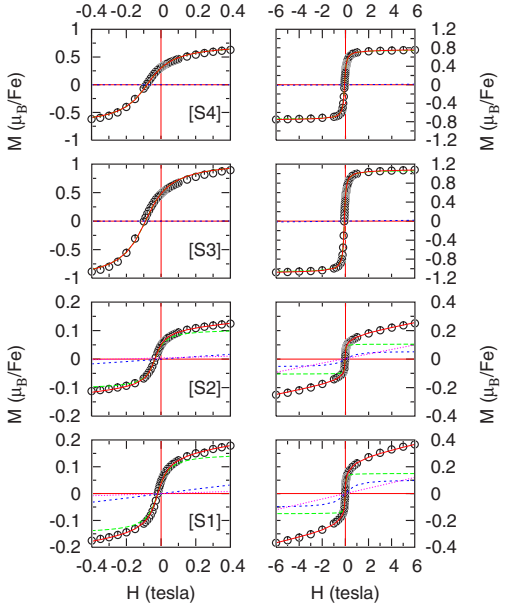

FIG. 5. (Color online) Only the part of data with descending magnetic field of the hysteresis loops measured at 5 K has been shown here for clarity. The experimental data are shown by open circles. The left panels show data in the expanded low field region −0.4–0.4 T for S1, S2, S3, and S4, and the right panel shows data in fields −6.0–6.0 T for the corresponding samples. For samples S1 and S2, the simulations are shown as the FM (long dash), the SPM (short dash), and the PM (dot) components and the sum (line). S3 and S4 are almost entirely FM (line).

50 K. Magnetic measurements on a ball-milled alloy of a similar composition showed[25] the Curie temperature to be ~200 K. In the present study, S3 and S4 are clearly ferromagnetic even at 300 K. In fact, a preliminary ^{57}Fe Mossbauer study of the S4 sample at room temperature has yielded a clear Zeeman sextet with a hyperfine field of about 24 T superimposed with a PM component. However, in the presence of strong ferromagnetism, no such PM component was required in the fitting of the magnetization data.

Table I shows that the values of the parameters related to the FM component increase with Fe content in samples from S1 to S3, and then decrease in S4. The reasons for this behavior are not clear, but it might be related to the change in Cu lattice upon alloying with Fe. It may be recalled that according to x-ray studies, there has been a lattice expansion from S1 to S3, and then a contraction in S4. Also, it has been checked that the magnetic properties of these samples are stable over a period of more than a year.

B. ^{63}Cu NMR studies

^{63}Cu NMR signals can only be obtained from the PM component of the alloy, or from unalloyed copper, if present in the sample. Experiments were performed with a Bruker MSL100 spectrometer at a magnetic field of 7.04 T at temperatures of 4–300 K. Figure 6 shows ^{63}Cu NMR spectra of S1, S2, S3, and S4 at different temperatures. The spectra were usually obtained using 90°-τ-90°-solid echo pulse sequence. S1 and S2 yield narrow single resonance lines

TABLE I. Ferromagnetic and superparamagnetic saturation magnetizations M_S^{FM} and M_S^{SPM}, respectively, remanence M_R^{FM}, coercivity H_C, the average magnetic moment μ, and susceptibility of the paramagnetic component C^{PM} for the FeCu nanostructured alloys, obtained from the analysis of magnetization data at 300 and 5 K.

Sample (at 300 K)	M_S^{FM} (μ_B/Fe)[a]	M_R^{FM} (μ_B/Fe)	H_C (Oe)	M_S^{SPM} (μ_B/Fe)	μ (μ_B)	C^{PM} (μ_B/Oe)
S1	0.043(5)	~0.0	~0.0	0.044(5)	1200(100)	$\sim 10^{-7}$
S2	0.055(5)	0.004(2)	30(10)	0.025(5)	1200(100)	$\sim 10^{-7}$
S3	0.96(2)	0.40(2)	760(30)			$\sim 10^{-7}$
S4	0.67(2)	0.24(2)	600(30)			$\sim 10^{-7}$
Sample (at 5 K)	M_S^{FM} (μ_B/Fe)	M_R^{FM} (μ_B/Fe)	H_C (Oe)	M_S^{SPM} (μ_B/Fe)	μ (μ_B)	C^{PM} (μ_B/Oe)
S1	0.150(5)	0.038(5)	203(20)	0.105(5)	18(3)	$2.0(1)\times 10^{-6}$
S2	0.105(5)	0.045(5)	340(20)	0.055(5)	18(3)	$1.6(1)\times 10^{-6}$
S3	1.07(2)	0.48(2)	900(40)			$\sim 10^{-7}$
S4	0.75(2)	0.30(2)	800(40)			$\sim 10^{-7}$

[a]Bohr magneton per Fe atom.

which, at any temperature, are broad compared to that from Cu metal nanoparticles. These spectra could be obtained by exciting the full spectrum with a single narrow radio-frequency (rf) pulse. The position and width of the resonance lines were obtained by fitting the spectra with a Lorentzian shape function. The widths of the resonance lines in S1 and S2 increase with a decrease in temperature. Also shown with S1 in Fig. 6 is the ^{63}Cu resonance line from Cu metal nanoparticles. The position and width of this resonance line are independent of temperature.

The dominant components of the signals from S3 and S4 are very much broad. These signals were recorded by sweeping the frequency in steps, in which a narrow region of the spectrum was excited by a suitable rf pulse. Normalized amplitude of the Fourier transformed time domain signal at each step was measured and plotted. Superimposed with the broad resonance lines in S3 and S4, a small narrow component is also obtained. Spectra of S3 and S4 were fitted as a sum of two components with Lorentzian shape. With lowering of temperature, the intensity of the narrow component is significantly reduced, but its width remains unchanged. The width of the broad component slightly increases at 4 K from that at 295 K.

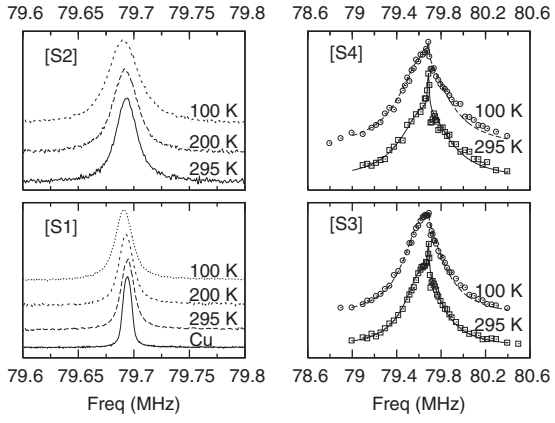

FIG. 6. ^{63}Cu NMR spectra at different temperatures for S1, S2, S3, and S4. For S3 and S4, the simulations of the spectra are shown as lines. Also shown with S1 is the temperature independent resonance line from Cu nanoparticles.

Spectral features suggest that the signals are obtained from the PM component of the FeCu alloys and there is no precipitation of unalloyed Cu. Moreover, the PM component remains undiminished down to 4 K even for S3 and S4 which are rather highly ferromagnetic. The two-component spectra may indicate that the alloys are not absolutely homogeneous and the narrow component could originate from paramagnetic copper in particles or clusters of low Fe content. However, at room temperature, the narrow components constitute less than 0.1% of the total area under the spectra and it may be said that the alloys are fairly homogeneous.

Studies of ^{63}Cu NMR were performed in several dilute magnetic alloys[26,27] of copper that exhibited the Kondo effect. Bulk FeCu alloys with Fe concentrations in the range of ~0.002–0.12 at. % have Kondo temperature of $T_K \approx 7$ K, independent of Fe content, and they were thoroughly studied by NMR.[26–29] These studies show that Fe induced broadening $\Delta\nu$ of the ^{63}Cu resonance linewidth in FeCu alloys is of magnetic origin. In the temperature range of the present experiment, the significant contributions to the broadening are from (1) the local field produced by the dipolar and indirect exchange coupling between ^{63}Cu nuclear spin and the localized moment of Fe ion and (2) the enhancement of the conduction electron spin polarization in the vicinity of Fe ions occurring much below T_K. The effect of small size may be discernible only for very small particles, ~5 nm, and at temperatures below about 5 K.[30] A comparison of the linewidths obtained in the present experiment with those in the above-mentioned literature shows that Fe content in the paramagnetic phase is ~0.02 at. % for S1 and ~0.04 at. % for S2.

Figure 7 shows the plot of the broadening $\Delta\nu/\nu_0$, where ν_0 is the position of reference for ^{63}Cu, against temperature

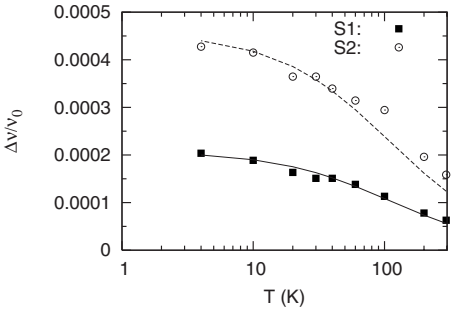

FIG. 7. The temperature dependence of Fe contribution to ^{63}Cu NMR linewidth $\Delta\nu/\nu_0$ in samples S1 and S2. ν_0 is the reference frequency of ^{63}Cu. The lines are theoretical fit as in the text.

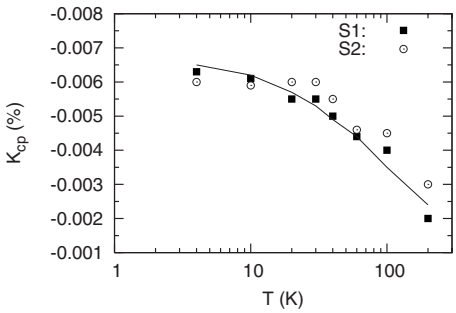

FIG. 8. The temperature dependence of Fe contribution to ^{63}Cu NMR Knight shift K_{cp} in samples S1 and S2. The line is the theoretical fit.

for S1 and S2 and the data could be satisfactorily fitted with

$$\Delta\nu/\nu_0 \propto (T+\theta)^{-1}, \tag{2}$$

where θ=110 K. In bulk FeCu alloys, the temperature dependence of linewidths at high fields were shown[27,28] to be comparable with the bulk susceptibility of the alloys showing a $(T+\theta)^{-1}$ variation,[31] where θ is related to Kondo temperature as $\theta=4.5T_K$. The value of θ obtained in the present case is obviously high compared to that of 29 K observed in bulk dilute FeCu alloys. However, this is about the minimum value of θ that could be obtained from the fitting, allowing all variations in the denominator of Eq. (2). This result indicates that the nanoparticles of dilute FeCu alloys might exhibit a higher Kondo temperature, e.g., ~24 K compared to bulk alloys.

With lowering of temperature, the spectra of all the samples shift toward the low frequency side, as seen in Fig. 6. In a magnetic alloy, the position of resonance of the host nonmagnetic nucleus can be written as[32]

$$\nu = \nu_0(1 + K_{ce} + K_{cp}). \tag{3}$$

In the above equation, $\nu_0 K_{ce}$ represents the shift in frequency due to the direct contact hyperfine interaction of the nucleus with *s*-character conduction electrons and is proportional to the conduction electron spin magnetization at the nuclear site. This term is positive and usually temperature independent as in Cu nanoparticles. The other term $\nu_0 K_{cp}$ is an indirect hyperfine interaction term due to the core polarization of the parent ion and is proportional to the spin magnetization of the parent ions core *s* electrons induced by polarized conduction electrons. $\nu_0 K_{cp}$, which, in the present case, is the Fe ion contribution to the shift in ^{63}Cu resonance position, was obtained by measuring the difference between the resonance frequency in alloy and that in Cu metal assuming that K_{ce} of Cu of 0.232% does not change upon alloying. Experimental and theoretical work suggest that a negative core polarization term is expected in 3*d* transition metal systems.[33] In bulk FeCu alloys, the observation of a positive temperature dependent Fe contribution to the Knight shift could not be satisfactorily explained.[29] In the present case, a negative K_{cp} results in the lowering of ^{63}Cu resonance frequency in FeCu alloys from that in Cu. Figure 8 shows the plot of K_{cp} against temperature for S1 and S2. The line in Fig. 8 corresponds to the equation $K_{cp} \propto (T+110)^{-1}$, which reasonably fits the data.

The broad NMR signals in S3 and S4 have not been analyzed. It is possible that in these samples, large resonance linewidth results from a much higher Fe concentration in the paramagnetic alloy phase compared to that in S1 or S2. However, as mentioned before (Fig. 6), the widths do not increase appreciably when temperature is lowered from 295 to 4 K. A similar magnitude of line broadening was obatined[34] in ^{63}Cu NMR study in ferromagnetic and/or nonmagnetic multilayers of iron and copper, and it was found to be resulting not from the RKKY interaction but from the stray field distribution from the rough Fe/Cu interface. In a similar way, if in S3 and S4 the ferro- and paramagnetic alloy phases coexist in close proximity, the magnetic field distribution due to the former may result in the large ^{63}Cu NMR linewidth in the latter as observed.

^{63}Cu spin-lattice relaxation rate $(1/T_1)$ was measured at temperatures of 4–300 K and at 7.04 T in S1 and S2. For S3 and S4, good measurements could be done only below 100 K. The results showed no significant difference in the temperature dependence of $1/T_1$ among the samples, i.e., all four alloys exhibit the Korringa-type relaxation behavior in which $1/T_1$ is proportional to temperature, almost identical to that in Cu metal. Studies in bulk FeCu samples showed[28] that the Fe contribution to the ^{63}Cu relaxation rate was enhanced between 4.2 and 1.4 K and decreased rapidly with increasing applied field between 0.25 and 1.5 T. Since the present samples seem to exhibit a higher Kondo temperature, it would be worthwhile to study the spin-lattice relaxation behavior in these samples at small magnetic fields and lower than liquid helium temperatures.

IV. CONCLUSION

FeCu granular alloys have been prepared and characterized by EDS, x-ray diffraction, and TEM studies. Magnetization measurements yield the blocking temperature distributions characteristic of small magnetic particles. The samples of lower Fe contents combine superparamagnetic and paramagnetic components, whereas the higher Fe containing samples are overwhelmingly ferromagnetic. ^{63}Cu NMR studies clearly show that in all four samples, unalloyed Cu is absent and a fraction of Fe is diluted in Cu giving rise to the

paramagnetic component having $\sim 0.02-0.04$ at. % Fe in Cu, and this component is retained even at low temperatures. The temperature dependence behavior of Fe contribution to ^{63}Cu NMR linewidth and Knight shift suggest that the paramagnetic component might exhibit a Kondo temperature of ~ 24 K that is much higher than that obtained in bulk dilute FeCu alloys.

ACKNOWLEDGMENT

The authors are thankful to their colleagues in the Chemical Science, Surface Physics and Biophysics divisions of SINP for helping in the sample preparation, EDS, and TEM studies.

[1] J. Q. Xiao, J. S. Jiang, and C. L. Chien, Phys. Rev. Lett. **68**, 3749 (1992).
[2] A. E. Berkowitz, J. R. Mitchell, M. J. Carey, A. P. Young, S. Zhang, F. E. Spada, F. T. Parker, A. Hutten, and G. Thomas, Phys. Rev. Lett. **68**, 3745 (1992).
[3] E. F. Kneller, J. Appl. Phys. **35**, 2210 (1964).
[4] C. L. Chien, S. H. Liou, D. Kofalt, W. Yu, T. Egami, and T. R. McGuire, Phys. Rev. B **33**, 3247 (1986).
[5] J. R. Childress, C. L. Chien, and M. Nathan, Appl. Phys. Lett. **56**, 95 (1990).
[6] M. B. Stearns and Y. Cheng, J. Appl. Phys. **75**, 6894 (1994).
[7] J. R. Childress and C. L. Chien, Phys. Rev. B **43**, 8089 (1991).
[8] S. Honda, M. Nawate, M. Tanaka, and T. Okada, J. Appl. Phys. **82**, 764 (1997).
[9] J. Eckert, J. C. Holzer, C. E. Krill III, and W. L. Jhonson, J. Appl. Phys. **73**, 2794 (1993).
[10] G. Mazzone and M. Vittori Antisari, Phys. Rev. B **54**, 441 (1996).
[11] R. L. Anton, M. L. Fdez-Gubieda, G. Kurlyandskaya, and A. Garcia-Arribas, J. Magn. Magn. Mater. **254-255**, 85 (2003).
[12] G. M. Chow, T. Ambrose, J. Q. Xiao, M. E. Twigg, S. Baral, A. M. Ervin, S. B. Qadri, and C. R. Feng, Nanostruct. Mater. **1**, 361 (1992).
[13] A. Yedra, L. F. Barquin, J. C. G. Sal, and Q. A. Pankhurst, J. Magn. Magn. Mater. **254-255**, 14 (2003).
[14] F. Bonet, S. Grugeon, L. Dupont, R. H. Urbina, C. Guery, and J. Tarascon, J. Solid State Chem. **172**, 111 (2003).
[15] J. Shen, Z. Li, Q. Yan, and Y. Chen, J. Phys. Chem. **97**, 8504 (1993).
[16] G. N. Glavee, K. J. Klabunde, C. M. Sorensen, and J. C. Hadjipanayis, Langmuir **8**, 771 (1992).
[17] I. Dragieva, D. Mehandjiev, E. Lefterova, M. Stoycheva, and Z. Stoynov, J. Magn. Magn. Mater. **140-144**, 455 (1995).
[18] J. J. Lu, H. Y. Deng, and H. L. Huang, J. Magn. Magn. Mater. **209**, 37 (2000).
[19] K. Zaveta, H. K. Lachowicz, M. Marysko, Z. Arnold, and P. Dluzewski, J. Alloys Compd. **392**, 12 (2005).
[20] J. R. Davis and T. J. Hicks, J. Phys. F: Met. Phys. **9**, L7 (1979).
[21] K. Sumiyama, T. Yoshitake, and Y. Nakamura, J. Phys. Soc. Jpn. **53**, 3160 (1984).
[22] V. K. S. Shante and S. Kirkpatrick, Adv. Phys. **20**, 325 (1971).
[23] P. Crespo, M. J. Barro, I. Navarro, M. Vasquez, and A. Hernando, J. Magn. Magn. Mater. **140-144**, 85 (1995).
[24] K. Racka, M. Gich, A. Slawska-Waniewska, A. Roig, and E. Molins, J. Magn. Magn. Mater. **290-291**, 127 (2005).
[25] E. Ma, M. Atzmon, and F. E. Pinkerton, J. Appl. Phys. **74**, 955 (1993).
[26] A. J. Heeger, L. B. Welsh, M. A. Jensen, and G. Gladstone, Phys. Rev. **172**, 302 (1968).
[27] H. Alloul, J. Darville, and P. Bernier, J. Phys. F: Met. Phys. **4**, 2050 (1974).
[28] J. E. Potts and L. B. Welsh, Phys. Rev. B **5**, 3421 (1972).
[29] T. Sugawara, J. Phys. Soc. Jpn. **14**, 643 (1959).
[30] W. P. Halperin, Rev. Mod. Phys. **58**, 533 (1986).
[31] J. L. Tholence and R. Tournier, Phys. Rev. Lett. **25**, 867 (1970).
[32] M. A. H. McCausland and I. S. Mackenzie, Adv. Phys. **28**, 305 (1979).
[33] J. A. Seitchik, V. Jaccarino, and J. H. Wernick, Phys. Rev. **138**, A148 (1965).
[34] J. Lu, P. L. Kuhns, M. J. R. Hoch, W. G. Moulton, and A. P. Reyes, Phys. Rev. B **72**, 054401 (2005).